



A GENUINELY MULTIDISCIPLINARY JOURNAL

CHEMPLUSCHEM

CENTERING ON CHEMISTRY

Accepted Article

Title: Rhodium Nanoparticles Supported on Hollow Nano-Mesoporous Spheres with Nitrogen-Doped Carbon: An Efficient Catalyst for the Reduction of Nitroarenes under Mild Conditions

Authors: Shihan Wang, Jinyu Dai, Zhiqiang Shi, Zeshan Xiong, Zongtao Zhang, Shilun Qiu, and Runwei Wang

This manuscript has been accepted after peer review and appears as an Accepted Article online prior to editing, proofing, and formal publication of the final Version of Record (VoR). This work is currently citable by using the Digital Object Identifier (DOI) given below. The VoR will be published online in Early View as soon as possible and may be different to this Accepted Article as a result of editing. Readers should obtain the VoR from the journal website shown below when it is published to ensure accuracy of information. The authors are responsible for the content of this Accepted Article.

To be cited as: *ChemPlusChem* 10.1002/cplu.201900657

Link to VoR: <http://dx.doi.org/10.1002/cplu.201900657>

WILEY-VCH

www.chempluschem.org



Rhodium Nanoparticles Supported on Hollow Nano-Mesosilica Spheres with Nitrogen-Doped Carbon: An Efficient Catalyst for the Reduction of Nitroarenes under Mild Conditions

Shihan Wang, Jinyu Dai, Zhiqiang Shi, Zeshan Xiong, Zongtao Zhang, Shilun Qiu, Runwei Wang*^[a]

Abstract: Using atomic efficiency, low temperature, low pressure, and a non-toxic hydrogen source as a reducing agent for reduction of nitroarenes were shown to be the most ideal reaction conditions. In this work, an efficient catalyst that Rh nanoparticles supported on hollow nano-mesosilica spheres with nitrogen-doped carbon was developed. Rh nanoparticles were stabilized and uniformly dispersed by nitrogen atoms, the inner N-doped carbon shell was used to adsorb reaction substrates and improve catalytic activity. The catalyst showed remarkable activity (maximum yield at 1.5 h) and selectivity (100%) for the reduction of nitrobenzene at low temperature (80 °C), atmospheric pressure (1 atm), and without base in the aqueous environment. Moreover, the hydrothermal stability of this nanocatalyst was better than other catalysts in boiling water at 100 °C for 48 h and effectively prevented the aggregation and leaching of Rh NPs during the reaction.

Introduction

The hydrogenation reduction of nitroarenes to aromatic amines is an important process often used to prepare fine chemical products such as agrochemicals, pharmaceuticals, pigments, and cosmetics.^[1] At present, iron powder reduction of nitrobenzene,^[2] and ammoniation of phenol^[3] or chlorobenzene^[4] are typically used to produce aromatic amine in industrial processes. However, relatively complex equipment, corrosive materials, low utilization rates of raw materials, harsh reaction conditions, many by-products, and related environmental problems are drawbacks of these protocols. Currently, using H₂ as a reducing agent is more atomically efficient, and transfer catalytic hydrogenation in mild conditions is used for the reduction of nitroarenes. Shimizu and co-workers recently used silver clusters on θ -Al₂O₃ for the catalyzed hydrogenation reduction of nitroarenes. This hydrogenation reaction utilized high pressure of H₂ (3 bars) as the reductant in THF at 160 °C.^[5] Catalytic hydrogenation using hydrogen gas usually requires high pressure equipment, which is typically accompanied with significant risk and toxic flammable solvents.^[6] Although transfer hydrogenation provides an attractive option for the reduction of nitroarenes, where hydrazine is used as the reducing agents, hydrazine is a challenge both technically and economically because of the cellular toxicity of hydrazine.^[7]

Ideal conditions for the hydrogenation of nitroarenes include no autoclaves, high atomic efficiency, and hydrogen as the reducing agent. However, these processes typically use homogeneous catalysts that are generally dissolved in the reaction medium, and the catalysts usually possess challenges such as difficult separation and an inability to recycle. Also, the metal residue remaining after the reaction can cause environmental pollution.^[8] When using a heterogeneous metal

catalyst, there are many obstacles of the catalytic process, such as high temperature or pressure.^[9] The focus of this article is the development of a nanocatalyst that combines the advantages of homogeneous catalysts (high efficiency) and heterogeneous catalysts (reusability). However, the search for a highly active, selective, and retrievable catalyst that can reduce nitroarenes under mild reaction conditions still remains an important research area.

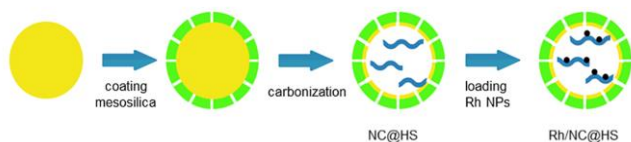
In recent years, it had been reported that hollow silica spheres loaded with metal nanoparticles were catalyzed, but agglomeration of metal nanoparticles under conventional reaction conditions (e.g., high temperature, high pressure, strong acidity or basic conditions) was considered to be one of the major limitations of catalysis.^[10] Multifunctional amphiphilic nanoreactors previously had studied in our group,^[11] owing to the anchoring effect of nitrogen atoms and the extreme stability of such an amphiphilicity, this nanoreactor exhibited excellent catalytic stability, which had greatly improved these defects.^[12] Herein, ultra-small Rh nanoparticles were loaded into NC@HS (hollow nano-mesosilica spheres with nitrogen-doped carbon) particles, where the Rh nanoparticles were stabilized by neighbouring surface nitrogen atoms. The inner N-doped carbon shell was used to adsorb reaction substrates and improve catalytic activity.^[13] We have compared the reaction of Pd under the same conditions on the same support in the experiment, we found that the reduction of nitrobenzene by such noble metals are all very efficient. This carrier had a universality of monodispersing into smaller nanoparticles, and it can obtain good reducing activity. But Pd had a lower resistance to sintering than Rh under hydrogen atmosphere. High dispersion Rh Nps possessed a high stability against sintering and they were more resistant to acid and alkali, so we chose the more stable metal-rhodium.^[14] The outer mesoporous silica shell was hydrophilic and able to disperse well in water and avoid flammable solvents. On the basis of these merits, this catalyst showed good activity, selectivity, and recyclability for the hydrogenation of aromatic compounds under pure water, no base, low temperature (80 °C) and atmospheric pressure (1 atm). The hydrogenation of nitroaromatic derivatives to the corresponding anilines was also studied. In addition, the carbon and silica composite support can effectively prevent the aggregation and leaching of Rh NPs during the reaction, so that the catalyst can maintain good stability over multiple cycles.

Results and Discussion

In Scheme 1, the synthesis of metal particles supported on the reported Rh/NC@HS (Rh-loaded hollow nano-mesosilica spheres with nitrogen-doped carbon) was carried out. Hollow nano-mesosilica spheres with nitrogen-doped carbon Rh/NC@HS were prepared via hydrothermal synthesis using the

[a] S. Wang, J. Dai, Z. Shi, Z. Xiong, Prof. Z. Zhang, Prof. S. Qiu, Prof. R. Wang
State Key Laboratory of Inorganic Synthesis and Preparative Chemistry, Jilin University
Changchun 130012 (P.R. China)
E-mail: rwwang@jlu.edu.cn

polymer precursor and TEOS as raw materials. The advantages of homogeneous catalysts – high efficiency – and heterogeneous catalysts – reusability – were combined to achieve Rh NPs loaded highly dispersedly into a double-sided shell material containing a coordination function of nitrogen atoms.



Scheme 1. Schematic of the synthesis process of Rh/NC@HS (Rh-loaded hollow nano-mesosilica spheres with nitrogen-doped carbon) particles.

Under the protection of the mesoporous silica shell, the inner polymer spheres were decomposed from the inside to the outside to form a hollow structure.^[15] The morphology of the Rh/NC@HS was observed by scanning electron microscopy (SEM) and transmission electron microscopy (TEM). The SEM image (Fig.1a) and TEM images (Figs.1b-d) show that each nanosphere has a uniform hollow structure with a diameter of about 300 nm and a shell thickness of about 30 nm. As shown in Fig.1d, Rh NPs indicated by red circle can be seen in the hollow structure. Rh NPs are uniformly dispersed in the porous nanoreactor and deposited on the NC@HS by a conventional impregnation-reduction method. Due to the effective exposure of multiple Rh NPs active sites, the catalyst exhibits unique catalytic properties for the hydrogenation reduction of nitroaromatics under mild reaction conditions. Figure 2a shows the particle size distribution of Rh NPs, where the average particle size was evaluated by randomly evaluating more than 100 Rh NPs, and the average diameter of the ultrafine Rh NPs was found to be 2.2 nm. Ultra-small Rh NPs were uniformly dispersed and non-aggregating due to the nitrogen stabilization and constrained effect of the NC@HS. The interaction between Rh NPs and the nitrogen-doped functionalized support (such as coordination and electron transfer) can decrease the metal particle mobility, improve the durability and stability, and effectively prevent the agglomeration or sintering of the particles, which can reduce efficiency.^[16]

The X-ray diffraction (XRD) pattern of Rh/NC@HS (Fig.S1) shows the typical reflections of nanoscopic crystalline Rh nanoparticles. The diffraction peaks at 2θ values of 41.1° , 47.8° , and 69.9° are ascribed to the (111), (200), and (220) planes of face-centered-cube (fcc) Rh, respectively. The XRD pattern after immobilization of Rh NPs shows no significant difference from the carrier, indicating that the structure of the nitrogen-doped crystal remained stable after the Rh particles were supported.

The structures of the Rh/NC@HS hollow spheres were further analyzed by N_2 adsorption-desorption. The surface area and

porosity of NC@HS and Rh/NC@HS were measured, and the isotherm (Fig.S2) showed a type I plus IV curve. There is a sharp increase in low relative pressure (0-0.01) and a high P/P_0 ratio in the range of 0.3-0.9, indicating the presence of microporous carbon and mesoporous silica in the material. A pressure ratio of 0.5-0.9 shows an H3 hysteresis loop, indicating a cavity structure inside the material. There were almost no changes in the isotherm and particle size distribution after Rh particle loading, indicating that the Rh particles did not block or change the pore structure. The carrier showed Brunauer–Emmett–Teller (BET) surface areas of $345.2610 \text{ m}^2/\text{g}^{-1}$ and pore size distributions of 0.7 nm and 1.3 nm (Fig.S3). This is important for metal particles dispersion and rapid diffusion of substrates during the catalytic process. This result is consistent with the TEM and XRD results.

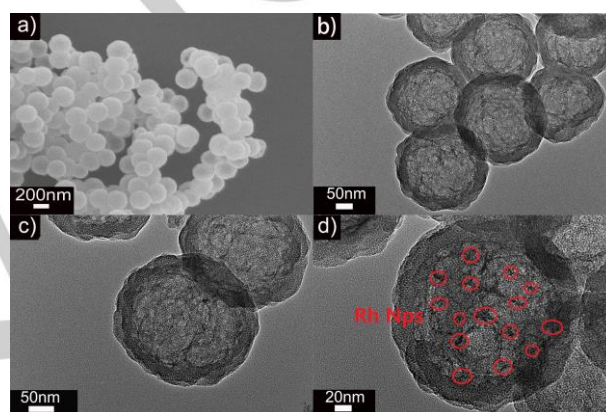


Figure 1. (a) SEM image, (b-d) TEM images of Rh/NC@HS.

X-ray photoelectron spectroscopy (XPS) concluded that the sample contained C, H, N, O, and Si. The state of the supported Rh NPs was also obtained by X-ray photoelectron spectroscopy. The Rh 3d XPS spectrum further illustrates that the surface Rh is mainly in the metallic state and the Rh 3d_{5/2} binding energy is located at 308.6 eV (Fig.S4). Compared to the Rh 3d_{5/2} peak position of commercial Rh/C (308.2 eV), the Rh 3d_{5/2} binding energy of the Rh/NC@HS is positively-shifted (Fig. S5).^[17] This slight deviation may be related to the weak interactions between Rh and N, nitrogen atoms not only anchored and stabilized Rh NPs, also played the role of dispersing charge. This conclusion is consistent with the XRD results. The high resolution XPS spectrum of N 1s (Fig.S6) can be decomposed into three peaks at 401.3 eV, 400.3 eV, and 399.2 eV, attributed to graphitic-N, pyrrolic-N, and pyridinic-N, respectively.

After stirring at room temperature, impregnation was sufficient and Rh NPs were immobilized on NC@HS via H_2 reduction. Assuming the effects of salt produced as a by-product, the use of $NaBH_4$ has been greatly reduced. The inductively coupled plasma atomic emission spectroscopy (ICP-AES) analysis confirmed that the Rh content of the catalyst was 1.238 wt.%.

The catalytic performance of Rh/NC@HS in the reduction of nitrobenzene to aniline was studied with H₂ as the reducing agent. The conditions of these catalytic experiments were very mild (atmospheric pressure H₂, 80 °C in clean water), where H₂ did not cause environmental pollution, and water was a readily available, safe, and environmentally friendly solvent.^[18] Prior to gas chromatography analysis, the catalyst was washed and removed by sonication, centrifugation, and the aqueous reaction mixture was extracted three times with ethyl acetate. Studies have shown that nitrobenzene does not react with NC@HS carriers, clearly demonstrating that Rh (0) particles are active sites. The catalyst exhibited higher activity (Table 1, entry 3) in aromatic reduction under mild solvent and pressure conditions,

where the turnover frequency (TOFS) was calculated to be 21.54 h⁻¹, and the optimal reaction time was considered to achieve complete conversion of the reactants. Even after longer reaction time, nitrobenzene was not reduced under these very mild conditions. Kinetic studies show (Fig. 2b) that the Rh/NC@HS achieved maximum yield at 1.5 h and showed good selectivity to aniline. The reaction order between 0-60 min was negative, this resulted from the far stronger adsorption of nitroarenes than that of H atoms. The yield and selectivity were studied at different temperatures, where only 7.3% yield was observed at 25 °C and 32% yield at 50 °C (Table 1, entries 1-2), indicating that 80 °C was the most desirable temperature.

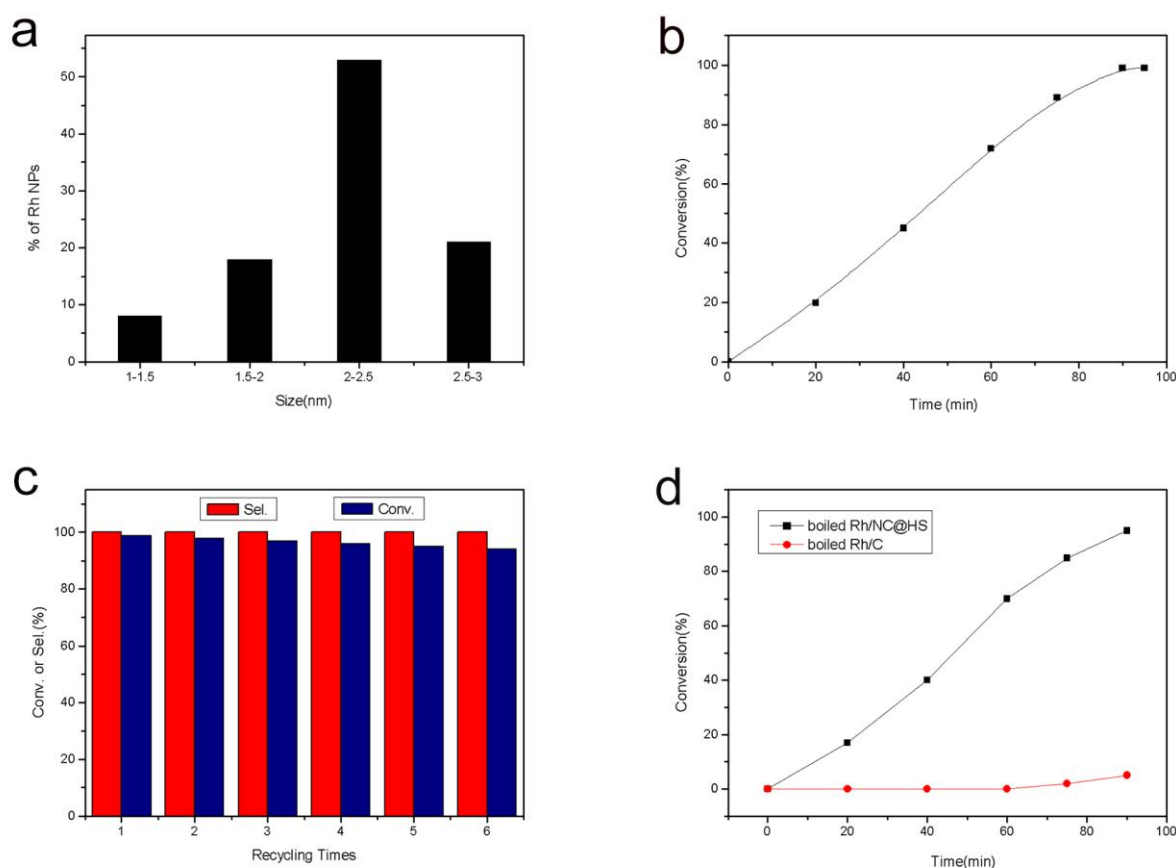


Figure 2. (a) Size distribution of Rh (0) NPs. (b) Time conversion plot for the reduction of nitrobenzene using Rh/NC@HS as a heterogeneous catalyst and (c) Recyclability of the catalyst Rh/NC@HS in the hydrogenation reduction of nitrobenzene. (d) Time-conversion plot for the reduction of nitrobenzene using boiled Rh/C and Rh/NC@HS as heterogeneous catalysts.

Rh/NC@HS not only exhibited good reducing properties in hydrogenating nitrobenzene but also exhibited strong reducing ability in hydrogenated reduction of nitroaromatics. In the reduction of *o*-nitrophenol and other substrates (Table 1, entries 4-13), the nitro group was easily reduced to the corresponding amino group, where both conversion and selectivity were greater than 90%. -OH (Table 1, entry 4) and -CH₂OH (Table 1, entry 8) groups were tolerated during the hydrogenation of NO₂. It is worth noting that the reaction time of the *o*-nitrotoluene was longer because the hydrogen bonding intramolecular interactions between the nitro group and the methyl group (Table

1, entries 5-7). Rh/NC@HS selectively hydrogenates the nitro group while other functional groups, such as C=O (Table 1, entry 9), C=C (Table 1, entry 10) are unaffected. This methodology was well tolerated to the electron-withdrawing substituents and found that 3-nitrostyrene (Table 1, entry 10) and *o*-chloronitrobenzene (Table 1, entry 11) both gave good selectivity (100%) of products. It also had excellent properties in 2-nitronaphthalene and 3-nitrophenyl (Table 1, entries 12-13). In conclusion, this catalyst shows high activity and selectivity for hydrogenation of challenging substrates, suggesting that

Rh/NC@HS is a versatile catalyst for selective hydrogenation of substituted nitroarenes.

We evaluated the general ability of Rh/NC@HS (2%) to catalyze the reduction of nitroaromatics and optimized the reaction conditions. When H₂ was used as the reducing agent, the nitrobenzene was almost completely converted in water after 1.5 h (Table S1, entry 1), but the reaction did not take place

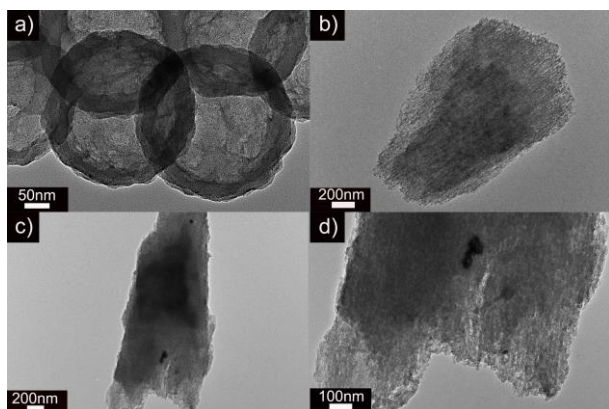


Figure 3. (a) TEM image of Rh/NC@HS recovered after the first reduction of nitrobenzene, (b) TEM image of commercial Rh/C, and (c, d) TEM images of Rh/C recovered after the first reduction of nitrobenzene.

without H₂ (Table S1, entry 2). The loading of metal Rh was reduced to 0.5%, but the reduction of nitrobenzene showed only a 20% yield (Table S1, entry 3). When 2% Rh Nps were supported on silica without N-doped carbon (Fig. 4a), they were partially aggregated in the hollow sphere (as shown in the red circle in the figure 4a). The catalytic efficiency of Rh @ HS was significantly reduced to 74% in the reduction of nitrobenzene (Table S1, entry 4). MCM-41 was used as the carrier and loaded with 2% Rh, since there was no fixation and dispersion of nitrogen, the conversion rate was only 66% when the reaction time was 1.5 h (Table S1, entry 5). This shows that the electron transferred from the Rh to N in the Rh/NC@HS, positive charges on the surface of Rh nanoparticles would be very favorable for activating nitro group. The interaction between Rh NPs and the nitrogen-doped functionalized support can decrease the metal particle mobility, improve the durability and stability, and effectively prevent the agglomeration or sintering of the particles. It has been reported that nitrogen-doped carbon shells without silicon shells were also stable^[11]. Conversion of nitrobenzene without the catalyst was as low as 0 in 1.5 h (Table S1, entry 6). There was almost no conversion of nitrobenzene at 1.5 h when the carrier NC @ HS was used as a catalyst (Table S1, entry 7), which verified that Rh NPs were the active sites.

The durability of the Rh/NC@HS catalyst was also tested because the recovery of the catalyst is important in industrial applications.^[19] For that purpose, nitrobenzene was subjected to a series of six consecutive hydrogenation reactions in water (Fig. 2c). The catalyst was easily removed from the reaction mixture by centrifugation and washing with water and ethanol, then reused under the same conditions. The catalyst exhibited high

efficiency and showed no significant loss in the hydrogenation of nitrobenzene. The actual Rh loading in the used Rh/NC@HS catalyst after six cycles was estimated to be 1.196 wt.% using ICP-OES, where there was no significant loss in Rh content. This indicated that the catalytic active sites were stable in the porous material (Fig. 3a), where the doping of nitrogen played the role of anchoring the metal particles and the double-sided shell acted as an encapsulant. Due to the high commercial value of Rh / C, we compared our material with Rh / C, the recyclability of commercial Rh/C (Fig. 3b) in the reduction of nitrobenzene in water was studied, and it was determined that Rh NPs were seriously lost.

or even aggregated (Figs. 3c-3d), and, as a result, the catalytic efficiency of the second cycle was significantly reduced. It further illustrates that the anchoring effect of nitrogen on rhodium in Rh/NC@HS allowed the catalyst to be recovered, greatly reducing the cost of the catalyst.

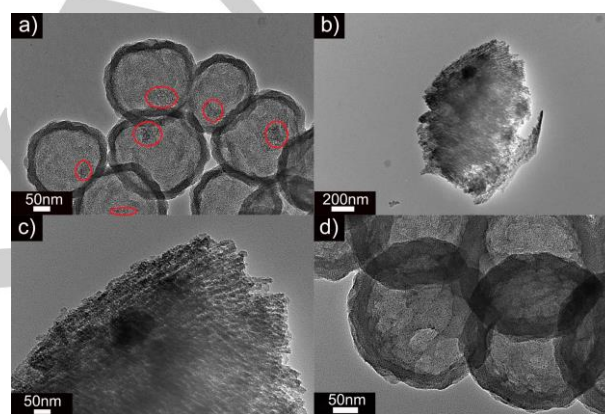
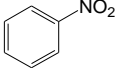
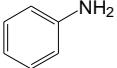
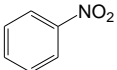
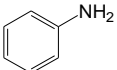
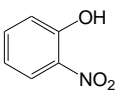
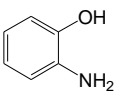
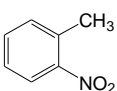
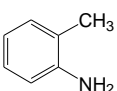
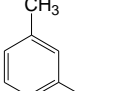
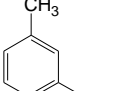
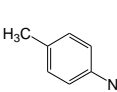
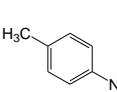
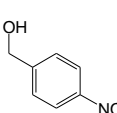
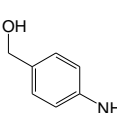
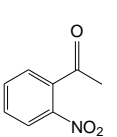
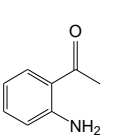
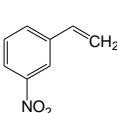
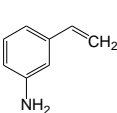
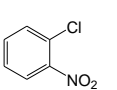
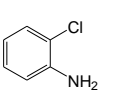
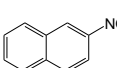
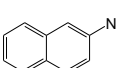
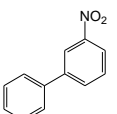
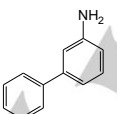


Figure 4. (a) TEM image of Rh@HS, (b, c) TEM images of boiled Rh/C, (d) TEM image of boiled Rh/NC@HS.

The hydrothermal stabilities of Rh/NC@HS, heated Rh/NC@HS, and Rh/C were verified for 48 h at 100 °C in boiling water. TEM images (Figs. 4b-4c) showed that Rh NPs on Rh/C were obviously lost, and the particle size was aggregated to 97.25 nm, while Rh/NC@HS had almost no change in morphology (Fig. 4d). Two heated samples were used to carry out the reduction of nitrobenzene (Fig. 2d). Rh/C lost most of its activity, while Rh/NC@HS maintained high activity and selectivity, confirming the continued stability of Rh/NC@HS.

Table 1. Hydrogenation of arenes with Rh/NC@HS in water^[a]

Entry	Substrates	Product	Temperature (°C)	Time (h)	Conv. (%) ^[b]	Sel. (%) ^[c]
1			25	1.5	7.3	99

2			50	1.5	32	100
3			80	1.5	>99	100
4			80	3	>99	95
5			80	8	>99	92
6			80	3	>99	98
7			80	3	>99	98
8			80	2	>99	93
9			80	1.5	>99	100
10			80	3	>99	100
11			80	3.5	>99	100
12			80	2	93	100
13			80	2	94	100

[a] Reaction conditions: Rh/NC@HS (50 mg, 2 wt% Rh, 0.01 mmol Rh), substrate (1 mmol), 4 mL water, 1 bar H₂.

[b] From GC measurement.

[c] Identified by GC-MS.

Conclusion

In summary, a heterogeneous synergistic reactor was designed with ultras-small Rh NPs to carry out the hydrogenation reduction of nitrobenzene, the carbon shell facilitated the adsorption of organic compound and the silica shell could utilize

water as a solvent. The superior catalytic performance was attributable to the preferential adsorption of the nitrogen atoms by the N-doped carbon and the synergistic effect of the active sites of the Rh nanoparticles. On this basis, the supported solid catalyst Rh/NC@HS showed high activity and selectivity, which may be related to its high specific surface area, nitrogen atoms, and ultra-small nanoparticles. In addition, this amphiphilic property was highly stable and showed good recyclability. This work not only provides a new strategy for the design of multifunctional nanoreactors but also brings more opportunities for green production of nitroaromatics.

Experimental Section

Materials

All chemicals were obtained from commercial suppliers and used as received. Hydrated RhCl₃·3H₂O, nitrobenzene, commercial Rh/C (5 wt.% Rh supported on carbon), polyvinyl pyrrolidone (PVP) were purchased from Aladdin Industrial Corporation. Formaldehyde, resorcinol, ethylenediamine, tetraethylorthosilicate (TEOS, 98%), and cetyltrimethylammonium bromide (CTAB, 99%) were purchased from Sinopharm Chemical Reagent Co. Ltd. H₂ was prepared from a high purity hydrogen generator.

Preparation of nano-mesoporous silica spheres with nitrogen-doped carbon (NC@HS)

Using traditional synthesis methods, deionized water (35 mL) and ethanol (15 mL) were well mixed, and CTAB (0.12 g) was dissolved in the mixed solution and stirred for 30 minutes. Subsequently, 0.16 mL of ethylenediamine (EDA), 0.16 g of resorcinol, and 0.24 mL of formaldehyde were added to the reaction mixture. The polybenzoxazine (PB) sphere was synthesized after stirring at room temperature for 2 hours. Then 2 mL of PVP-10 solution was added at a concentration of 12.8 g/L. Next, CTAB (50 mg) and TEOS (0.6 mL) were added to synthesize mesoporous silica shell to coat the newly formed semi-finished solution. The reaction was carried out at room temperature with continuous stirring. After four hours, the composites were collected by centrifugation, washed several times with ethanol and deionized water, dried under ambient conditions for two days, and ground into powder to obtain the product. Finally, the obtained product was subjected to pyrolysis (the pyrolysis temperature was increased to 600 °C from 30 °C, where the heating rate was increased by 5 °C per minute, and 600 °C was maintained for 4 hours) under an argon atmosphere to obtain the final product NC@HS.

Preparation of Rh/NC@HS

The catalysts were prepared at 2 wt% Rh using NC@HS as the support. An aqueous solution of the metal precursor was prepared by dissolving RhCl₃·3H₂O (250 mg) in water (100 mL) at room temperature. The appropriate amount of support was placed in a round-bottom flask containing 40 mL of water and sonicated for 30 minutes. Then a few drops of RhCl₃·3H₂O solution was added to obtain the desired metal loading with magnetic stirring at room temperature. After sorption of the Rh solution, the solvent was removed by rotary evaporation. The composites were reduced at 200 °C in a mixed atmosphere of 5% H₂ and 95% N₂ for 2 hours and heated at a rate of 5 °C/min to obtain the final catalyst Rh/NC@HS.

Characterization

Scanning electron microscopy (SEM) measurements were performed on a JEOL JSM-6700F field-emission electron microscope. Transmission electron microscopy (TEM) images were carried out using a FEI Tecnai G2 F20s-twin D573 field emission transmission electron microscope at 200 kV. The crystal structures were determined by a Rigaku 2550 X-ray diffractometer (XRD) equipped with a Cu K α irradiation source. N₂ adsorption-desorption isotherms were recorded using a Micromeritics ASAP 2010 sorptometer at -196 °C. Before performing the measurements, all samples were degassed at 120°C for a minimum period of 12 h. The specific surface area of the solid material was calculated by the conventional Brunauer-Emmett-Teller (BET) method from the linear portion of the BET plot. Pore size distribution was estimated from the adsorption branch of the isotherm by the DFT method. Raman spectroscopy was performed using a Horiba LabRAM HR Evolution. Inductively coupled plasma mass spectrometry (ICP) analyses were carried out on a NexION 350 ICP-MS instrument. The X-ray photoelectron spectroscopy (XPS) was performed using an ESCALAB250 spectrometer.

Hydrogenation of nitrobenzene

In the traditional catalytic reduction process, a certain amount of catalyst (Rh/NC@HS) was placed in a 50 mL round bottom flask and 4 mL of deionized water was added. The catalyst was fully dissolved in water by ultrasonic vibration, and 0.5 mmol of nitrobenzene was added. The closed system was evacuated and communicated with a H₂ balloon. The reaction was carried out under magnetic stirring and refluxed in an 80 °C oil bath. After the reaction, the reaction mixture was extracted three times with 4 mL of ethyl acetate. The catalyst was recovered by centrifugation and washed several times with water and ethanol and directly used for the next catalytic cycle. The liquid phase was then analysed by GC-MS.

Acknowledgements

This work was supported by the National Natural Science Foundation of China (21390394, 21771082, 21771081, and 21703128), the National Basic Research Program of China (2012CB821700 and 2011CB808703), Natural Science Foundation of Jilin Province (20190201207JC) and the "111" project (B07016).

Conflict of Interest

The authors declare no conflict of interest.

Keywords: Heterogeneous catalysis, hydrogenation, nanostructures, silica, rhodium

- [1] a) R. Downing, P. Kunkeler, H. Bekkum, *Catal. Today* **1997**, *37*, 121-136; b) F. Heaney, *Synthesis* **2001**, *2001*, 2528-2528; c) X. Li, Z. Wang, S. Mao, Y. Chen, M. Tang, H. Li, Y. Wang, *Chin. J. Chem.* **2018**, *36*, 1191-1196.
- [2] J. Chen, D. Wang, J. Qi, G. Li, F. Zheng, S. Li, H. Zhao, Z. Tang, *Small* **2015**, *11*, 420-425.
- [3] X. Cui, H. Li, M. Yuan, J. Yang, D. Xu, Z. Li, G. Yu, Y. Hou, Z. Dong, *J. Colloid Interface Sci.* **2017**, *506*, 524-531.
- [4] J. Lyu, J. Wang, C. Lu, L. Ma, Q. Zhang, X. He, X. Li, *J. Phys. Chem. C* **2014**, *118*, 2594-2601.
- [5] K.-i. Shimizu, Y. Miyamoto, A. Satsuma, *J. Catal.* **2010**, *270*, 86-94.
- [6] M. Takasaki, Y. Motoyama, K. Higashi, S.-H. Yoon, I. Mochida, H. Nagashima, *Org. Lett.* **2008**, *10*, 1601-1604.
- [7] a) J. Zhou, Y. Li, H.-b. Sun, Z. Tang, L. Qi, L. Liu, Y. Ai, S. Li, Z. Shao, Q. Liang, *Green Chem.* **2017**, *19*, 3400-3407; b) P. Luo, K. Xu, R. Zhang, L. Huang, J. Wang, W. Xing, J. Huang, *Catal. Sci. Technol.* **2012**, *2*, 301-304.
- [8] F. L'epplattenier, P. Matthys, F. Calderazzo, *Inorg. Chem.* **1970**, *9*, 342-345.
- [9] a) M. Tamura, N. Yuasa, Y. Nakagawa, K. Tomishige, *Chem. Commun.* **2017**, *53*, 3377-3380; b) R. Gao, L. Pan, Z. Li, X. Zhang, L. Wang, J.-J. Zou, *Chin. J. Catal.* **2018**, *39*, 664-672.
- [10] G. C. Bond, *Chem. Soc. Rev.* **1991**, *20*, 441-475.
- [11] a) J. Dai, H. Zou, Z. Shi, H. Yang, R. Wang, Z. Zhang, S. Qiu, *ACS Appl. Mater. Interfaces* **2018**, *10*, 33474-33483; b) H. Zou, J. Dai, R. Wang, *Chem. Commun.* **2019**, *55*, 5898-5901.
- [12] a) Y. Cao, S. Mao, M. Li, Y. Chen, Y. Wang, *ACS Catal.* **2017**, *7*, 8090-8112; b) S. Mao, C. Wang, Y. Wang, *J. Catal.* **2019**, *375*, 456-465.
- [13] a) L. Chen, L. Zhang, Z. Chen, H. Liu, R. Luque, Y. Li, *Chem. Sci.* **2016**, *7*, 6015-6020; b) Z. Li, J. Liu, C. Xia, F. Li, *ACS Catal.* **2013**, *3*, 2440-2448; c) Z. Wei, J. Wang, S. Mao, D. Su, H. Jin, Y. Wang, F. Xu, H. Li, Y. Wang, *ACS Catal.* **2015**, *5*, 4783-4789.
- [14] M. Machida, Y. Uchida, Y. Ishikawa, S. Hinokuma, H. Yoshida, J. Ohyama, Y. Nagao, Y. Endo, K. Iwashina, Y. Nakahara, *J. Phys. Chem. C* **2019**, *123*, 24584-24591.
- [15] a) X. Fang, S. Liu, J. Zang, C. Xu, M.-S. Zheng, Q.-F. Dong, D. Sun, N. Zheng, *Nanoscale* **2013**, *5*, 6908-6916; b) X. Fang, J. Zang, X. Wang, M.-S. Zheng, N. Zheng, *J. Mater. Chem. A* **2014**, *2*, 6191-6197.
- [16] W. Qi, D. Su, *ACS Catal.* **2014**, *4*, 3212-3218.
- [17] a) J. Fierro, J. Palacios, F. Tomas, *Surf. Interface Anal.* **1988**, *13*, 25-32; b) A. Talo, J. Lahtinen, P. Hautojärvi, *Appl. Catal., B* **1995**, *5*, 221-231.
- [18] a) H. C. Hailes, *Org. Process Res. Dev.* **2007**, *11*, 114-120; b) D. Prat, A. Wells, J. Hayler, H. Sneddon, C. R. McElroy, S. Abou-Shehada, P. J. Dunn, *Green Chem.* **2015**, *18*, 288-296.
- [19] D. J. Cole-Hamilton, R. P. Tooze, *Springer Science & Business Media* **2006**.

Rhodium nanoparticles supported on hollow mesoporous silica spheres with nitrogen-doped carbon were used as nanoreactors (see figure). They exhibited excellent conversion and selectivity in hydrogenation reduction of nitroaromatics under mild conditions. Furthermore, owing to the anchoring effect of nitrogen atoms, the hydrothermal stability was better than other catalysts in boiling water for 48 h and effectively prevented the aggregation and leaching of Rh Nps during the reaction, so that the catalyst can maintain good stability over multiple cycles.



Shihan Wang, Jinyu Dai, Zhiqiang Shi,
Zeshan Xiong, Zongtao Zhang, Shilun
Qiu, Runwei Wang*

Page 1. – Page 6.

**Rhodium Nanoparticles Supported
on Hollow Nano-Mesosilica Spheres
with Nitrogen-Doped Carbon: An
Efficient Catalyst for the Reduction
of Nitroarenes under Mild
Conditions**